J Fluoresc (2008) 18:1115–1122
DOI 10.1007/s10895-008-0361-y

ORIGINAL PAPER

Surface Modified Single Molecules Free-Diffusion Evidenced by Fluorescence Correlation Spectroscopy

Céline Boutin · Rodolphe Jaffiol · Jérôme Plain · Pascal Royer

Received: 6 February 2008 / Accepted: 27 February 2008 / Published online: 18 March 2008

Abstract We report on the free diffusion of single molecule near an interface studied using fluorescence correlation spectroscopy. In particular, we show that the chemical nature of the substrate may modify the free diffusion of a widely used molecule (rhodamine 6G), thus inducing unexpected effects in fluorescence correlation spectroscopy measurements. Our results show a strong influence, up to a few micrometer from the interface, of the surface polarity. This effect is assessed through the relative weight of the two dimensions diffusion process observed close to the surface. Our results are discussed in terms of competition between surface-solvent, solvent-molecule and molecule-surface specific interactions.

Keywords Fluorescence correlation spectroscopy (FCS) · Single-molecule spectroscopy · Diffusion near interface

Introduction

Single molecule spectroscopy in solution consists in using fluorescent molecules (i.e. dyes) as a highly sensitive probe of specific dynamic processes. About their detection, it is essential to have the probability of finding a molecule in the optical observation volume significantly inferior to unity. This can be achieved by sufficiently diluting the molecule of interest and also by limiting the detection to a small volume. Thus the popular success of single molecule detection in solution during the last 10 years is directly linked to fluorescence correlation spectroscopy (FCS) developments [1–3]. Most of the recent FCS experiments were carried out with a confocal detection scheme, to decrease the probe volume to the diffraction limit. In practice, with typical high numerical aperture objective (NA=1.2), the limited confocal volume is smaller than a femtoliter (typically ≈0.2–0.5 μm^3) and can be approximated by an ellipsoid elongated along the optical axis, as schematically represented in Fig. 1 [4, 5]. However, with such "usual" FCS setup, it is only possible to work at nanomolar concentration range (from sub-nM to ≈50 nM). Moreover, occasionally it requires the use of ultra pure solvents to decrease as much as possible the background signal (Raman scattering, auto-fluorescence of living cells, …). This enlightens the experimental difficulties, especially in the case of biological in vivo or in vitro studies where "ideal" ultra pure conditions can not be met, and where the concentration of biomolecules is micromolar (mM) or higher. Different techniques have been recently proposed to strongly reduce the size of the observation volume, expanding the working range of single molecule experiments to biologically relevant concentration together with a significant decrease of the background. The first one is based on confocal total-internal-reflection fluorescence microscopy [6–10]. Another promising technique propose the implementation of a nano-illumination through a subwavelength aperture milled in a thin metallic film, sometimes named zero-mode waveguide [11–16]. The most important aspect of those new methods is the confinement of the excitation light, which is directly related to evanescent waves produced on the substrate–water interface (typically the depth of field is below 50 nm). Such new approaches point out the crucial problem related to molecular diffusion close to a surface, such as possible

C. Boutin · R. Jaffiol (✉) · J. Plain · P. Royer
Laboratoire de Nanotechnologie et d'Instrumentation Optique,
LRC CEA, ICD CNRS FRE2848,
Université de Technologie de Troyes,
12 rue Marie Curie, BP2060,
10010 Troyes cedex, France
e-mail: rodolphe.jaffiol@utt.fr

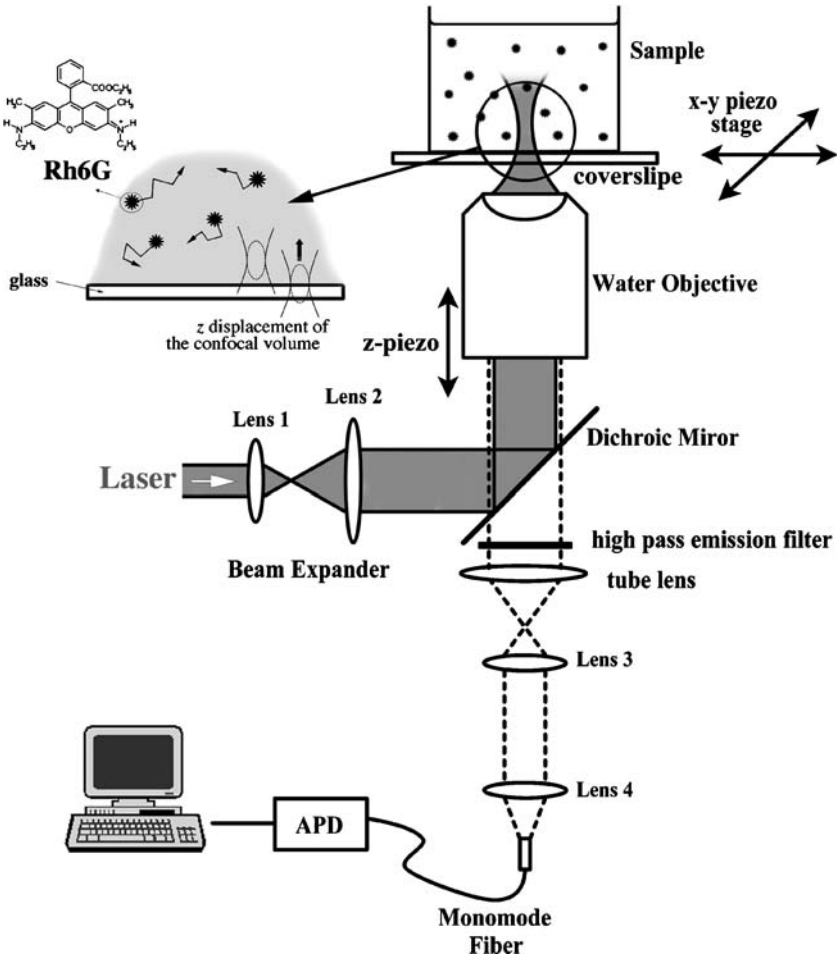

Fig. 1 Schematic representation of the experiment. A well, which contains a nanomolar solution of Rhodamine 6G (≈500 μl), is deposited on a glass substrate. FCS measurements are done according to a nano-controlled axial displacement of the confocal observation volume

interactions between the surface and the molecules of interest. Then, two essential questions arise. First, can surface perturb the system studied (lipids, proteins or some other constituents of plasma membrane for example)? Second, how the perturbation operates?

In this paper, we study how the chemical nature of the surface may play on the diffusion of dye molecules and induce unexpected effects on FCS measurements. By analyzing molecule of Rhodamine 6G (Rh6G) freely diffusing near a glass–water interface, as illustrated in Fig. 1, we probe all the specific interactions between molecule, surface and solvent. Thus, we propose to control precisely the chemical surface termination through a chemical functionalization of the glass substrate. As a consequence, the free diffusion of the Rh6G molecules is strongly modified depending on the polarity of the functionalized substrate. These new results suggest that FCS measurements near an interface, independently of the excitation type (i.e. evanescent waves, confocal…), could be strongly influenced by the chemical nature of the interface and that their interpretations could be altered by chemical interactions near the interface.

Materials and methods

Fluorescence correlation spectroscopy

Fluorescence correlation spectroscopy (FCS) is an experimental technique using statistical analysis of the fluctuations of fluorescence in order to decipher molecular dynamic events, such as diffusion or rotational fluctuations [17, 18]. FCS is based on the temporal autocorrelation of the collected fluorescence signal $F(t)$, emitted by the dyes diffusing through the optical detection volume which is limited by the laser beam focusing and the confocal detection. The autocorrelation $G(\tau)$ is evaluated as following [2, 19]:

$$G(\tau) = \frac{\langle F(t)F(t+\tau)\rangle}{\langle F(t)\rangle^2} = 1 + \frac{\langle \delta F(t)\delta F(t+\tau)\rangle}{\langle F\rangle^2} \qquad (1)$$

where $\delta F(t)$ is the fluctuation of the measured fluorescence $F(t)$ from the average value <F(t)>, i.e. $\delta F(t) = F(t) - < F(t) >$. As it can be seen in Eq. 1, one usually

considers the dynamic of the fluorescence fluctuations $\delta F(t)$ in an open sampling volume of a macroscopic system that fluctuates around average equilibrium concentration. The fluctuation of the concentration of each species is globally ruled by diffusion of each species in and out the optical probe volume. Assuming that the fluorescence fluctuations are globally related to the concentration fluctuations, FCS appears as a promising spectroscopic technique to investigate the molecular motion, such as free diffusion and molecular transport [20, 21]. However, other processes have to be considered, because they can induce new sources of fluorescence fluctuations. For example, we should consider the electronic molecular dynamics of dye molecules, such as singlet–triplet interactions. Schematically, the autocorrelation function curve $G(\tau)$ presents different temporal areas, each ones connected to specific physico-chemical processes [2, 17–19]. At long time scale, typically beyond 10 μs, the physical process which controls the evolution of $G(\tau)$ is the diffusion. Moreover, in this long time range, the amplitude of the autocorrelation function is inversely proportional to the average number of fluorescent molecules (noted N) in the optical observation volume. This feature imply to work under strong dilution condition to increase the signal-to-noise ratio. Additionally, the $G(\tau)$ decay time (namely diffusion time, noted τ_d) is derived from the translational diffusion coefficient D and the lateral size of the detection volume ω_0, according to the relation: $\tau_d = \omega_0^2/4D$ (typically $\omega_0 \approx 250$–300 nm with a high numerical aperture microscope objective) [2, 19]. The decay time τ_d corresponds in fact to the average time required for the fluorescent molecules to cross the detection volume. The evaluation of N and τ_d constitutes the two types of measurements, which provide the greatest interest for the present study. The variation of these two last parameters allows us to understand how the chemical nature of a surface may play on the diffusion of single molecule in a medium, particularly water.

Experimental setup

Our optical device for FCS measurement is based on a standard backscattering confocal microscope (a modified IX70 Olympus inverted microscope), as schematically presented in Fig. 1. The excitation light is provided by the 488 nm argon laser line. After passing through a beam expander (lens 1 and 2), the laser is reflected by a dichroic mirror (Semrock FF495-Di02) and strongly focused through a water immersion objective (Olympus UPlanSApo 60×/1.2 W). This setup is designed for probing very small confocal volumes by controlling the spatial extend of the laser beam at the entrance pupil of the objective and the size of the pinhole detector ($V \approx 0.3$ μm^3, experimentally determinated by measuring the average number of molecules, N, for several well known concentrations of Rh6G, data not presented). The fluorescence emission is collected through the same objective and passes through a sharp high pass filter over 500 nm (Semrock LP02-488RU). According to the total magnification of our microscope, M=15 (60× for the water objective and 0.25 for the additional optical imaging part comprise lenses 3 and 4, see Fig. 1), a monomode optical fibre with a core diameter of 9 μm is used as point detector for the confocal detection [22]. Optical fibres have two important advantages: first, the fibre core offers a natural small circular aperture; second, it allows us to send the fluorescence signal on the optical detector. Finally, the fluorescence signal is recorded with an avalanche photodiode (Perkin Elmer SPCM-AQR-16), with high quantum efficiency in the visible range and a low dark count rate (≈25 counts/s), connected to a homemade single photon counting module. This acquisition module (Phonos) is capable of distinguishing the photon counts with a resolution time better than the APD's dead time [5]. A computational multi-τ procedure calculates the autocorrelation functions $G(\tau)$ with a quasi-geometrical progression of the lag time from 0.2 μs to 3.3 s [23]. A fine achievement of the axial observation volume position is provided with a z-piezo device supporting the objective (PIFOC stage from Physik Instrumente). For a nanomolar solution of Rh-6G freely diffusing in water far from the interface, our FCS setup gives a diffusion time τ_d=44 μs with a high count rate per molecule (CRM), around 50 kHz, according to a laser power ≈100 μW measured at the entrance pupil of the objective.

Sample preparation

Three different surfaces have been produced to control the polarity degree, over a large range, at the glass–water interface.

Samples n°1 and n°2 have been prepared through the silanisation process (–CH_3 and –NH_2 terminated silanes, respectively) [24, 25]. The process requires high purity of all reagents and extreme cleanliness of the substrates and coverglass. The following chemicals were of the highest grade and used as received: anhydrous toluene, toluene and ethanol (HPLC grade, ACROS); 3-aminopropyldimethylethoxysilane (APDES, 97%), undecyltrichlorosilane (UDTS 97%) (ABCR/Gelest). The coverglass were cleaned thoroughly by immersion into freshly prepared *Piranha* solution [H_2SO_4/H_2O_2, 98%:30%; 2:1 (*v*/*v*)] for at least 30 min, extensively rinsed with deionized water, and dried in an oven. The glass substrates were immersed for 24 h in a 1% solution of the silane in anhydrous toluene under argon atmosphere. After washing with a solvent sequence (toluene, ethanol) the substrates were sonicated in toluene, which yielded high-quality silane monolayers.

Sample n°3 is a silanol surface (–OH terminated). It was obtained by immersing the glass substrate into freshly prepared Piranha solution [H_2SO_4/H_2O_2, 98%:30%; 2:1 (*v*/*v*)] for at least 30 min, extensively rinsed with deionized water, and dried in an oven.

Water contact angles were measured under ambient atmosphere at room temperature by using the sessile drop method and an image analysis of the drop profile with a home made system. Water contact angles were in agreement with expected values [25]. Indeed, we found 106°±0.5°, 67°±0.3° and 3°±0.3° for the sample 1, 2 and 3, respectively.

Results

Autocorrelation functions analysis

FCS measurements were performed on the three samples and a typical bare coverglass. Each autocorrelation function results from an average of three functions, recorded consecutively, each ones during 20 s. All the following results were obtained with a laser excitation power ≈100 μW, measured at the back pupil of the water objective. All the samples were covered with a nanomolar solution of Rh-6G in ultrapure water. To demonstrate the influence of the surface hydrophobicity on molecular diffusion process, we examined the evolution of the autocorrelation curves $G(\tau)$ in regards to the distance z from the glass–water interface, as schematically shown in Fig. 1. The confocal volume is initially positioned at the glass–solution interface in order to include the surface, and then slowly moved away from the interface using the z-piezo stage. For each z-position of the observation volume, FCS analyses were performed. A typical evolution of the autocorrelation curve, recorded on a bare coverglass, is presented in Fig. 2. Each curves were fitted with a standard formula describing the simultaneously translational diffusion of both a slow (2D) and a fast (3D) components, according to molecules diffusing in two-dimensions and in three-dimensions, respectively [2, 19]:

$$G(\tau) = 1 + \left\{1 + \frac{F\exp^{-\frac{\tau}{\tau_b}}}{1-F}\right\} \times \left\{\frac{N^{\text{slow}}}{\left(N^{\text{fast}}+N^{\text{slow}}\right)^2}\left(1+\frac{\tau}{\tau_d^{\text{slow}}}\right)^{-1} + \frac{N^{\text{fast}}}{\left(N^{\text{fast}}+N^{\text{slow}}\right)^2}\left(1+\frac{\tau}{\tau_d^{\text{fast}}}\right)^{-1}\left(1+\frac{\tau}{S^2\tau_d^{\text{fast}}}\right)^{-\frac{1}{2}}\right\} \quad (2)$$

The first term in Eq. 2 depicts, for a fraction F, the Rh6G molecules in a non-fluorescent state, which appears for singlet–triplet transitions kinetics [26], or also for surface association/dissociation process [27]. The characteristic time connected to such non-radiative processes is named τ_b. The second term describes the 2D diffusion of dyes at

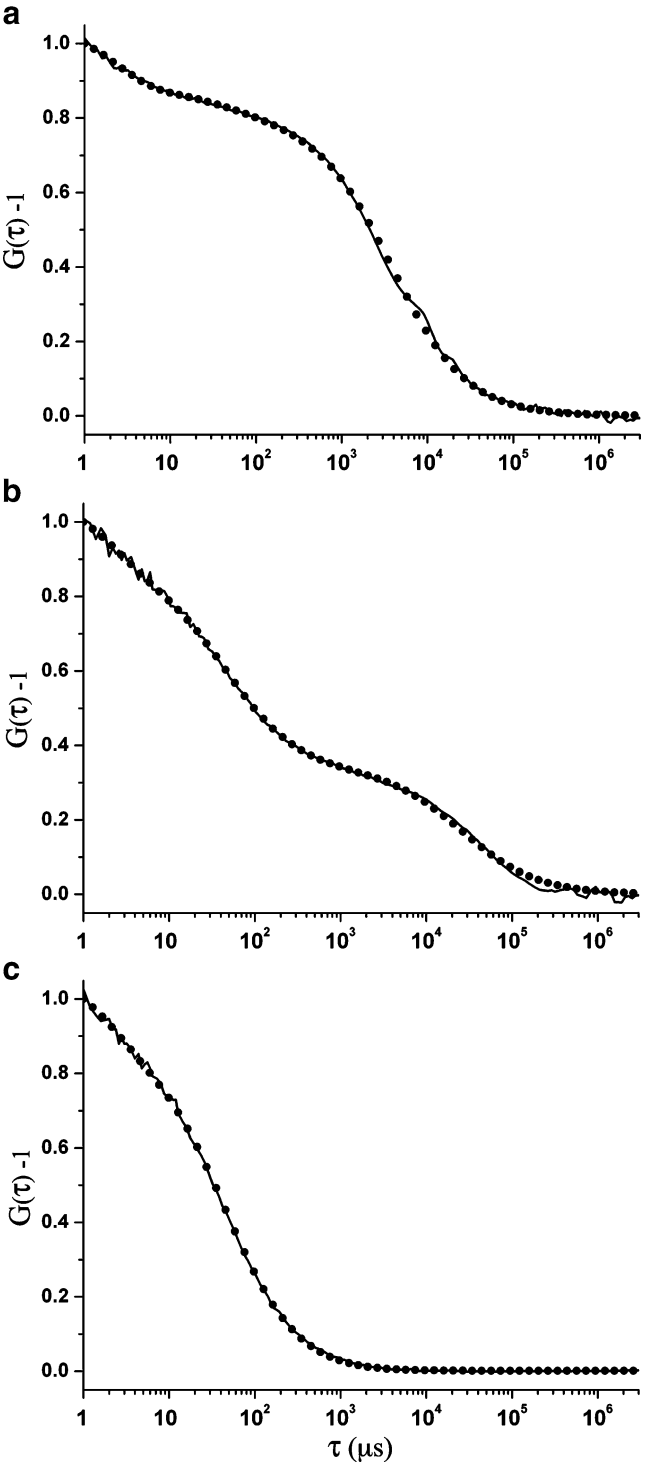

Fig. 2 Three normalized autocorrelation functions $G(\tau)$ obtained under a bare coverglass at different relative distance z from the interface. **a** z=0.25 mm, **b** z=0.75 μm and **c** z=4.25 μm. *Solid curves* the experimental autocorrelation curve. *Dot curves* the total fit according to Eq. 2

the vicinity of the glass–water interface [28]. The last term represents the contribution of Rh6G molecules freely diffusing at three dimensions in water. We use the subscript *slow* and *fast* to identify all the parameters related to this 2D diffusion and 3D diffusion, respectively. N^{slow} and N^{fast} are the average numbers of diffusing molecules through the confocal volume for each class of molecules. τ_d^{slow} and τ_d^{fast} are their respective diffusion times. The factor S represents the axial elongation of the confocal volume (S is typically ≈5). Therefore we are able to evaluate N^{slow} and N^{fast} from individual autocorrelation curves with the described fit model, Eq. 2, by fixing S and τ_d^{fast} obtained from of Rh6G freely diffusing in water far from the interface (z≈10–15 μm), $\tau_d^{fast} = 44\ \mu s$ and S=5. Figure 2 points out the typical axial evolution of the autocorrelation curves $G(\tau)$ recorded on a bare coverglass. Moreover, we can observe a very good accordance between experimental autocorrelation curves and their fit (all autocorrelation functions were evaluated by a standard least squares fitting procedure).

Accurate determination of the glass–water interface position

According to the fact that 2D diffusion of Rh6G only occurs at the glass–water interface, it is possible by using the so-called "Z-scan" method, previously proposed by A. Benda et al., to identify exactly the axial position of the interface, i.e. the surface where the Rh6G molecules diffuse in 2D [29, 30]. The Gaussian beam profile of the laser focusing gives rise to a z-dependence of the diffusion time τ_d^{slow} [29]. The minimum value of τ_d^{slow} is given for the smallest size of the beam radius, namely the beam waist ω_0. The obtained values of τ_d^{slow} in the case of the $-CH_3$ surface (sample 1) were plotted versus the relative focus position z, Fig. 3. As indicated on the plot, we observe a decrease followed in an increase of the diffusion time and the minimum can be easily obtained with a precision better than the axial increment, 0.25 μm. In our cases, the number of molecules diffusing near the glass–water interface is high enough [31], the minimum of τ_d^{slow} occurs together with a maximum of the fluorescence signal $F(t)$ and a maximum of its fluctuations $\delta F(t)$, as shown in Fig. 3. By this way, we can evaluate precisely the axial position of the glass–water interface for all the samples.

Influence of the chemical nature of the glass–water interface

Figure 4 shows the evolution of the normalized value of both mean concentrations C^{fast} and C^{slow} of diffusing molecules, in regards to the actual distance z of the observation volume from the interface. We examined the three samples previously presented, plus a bare coverglass.

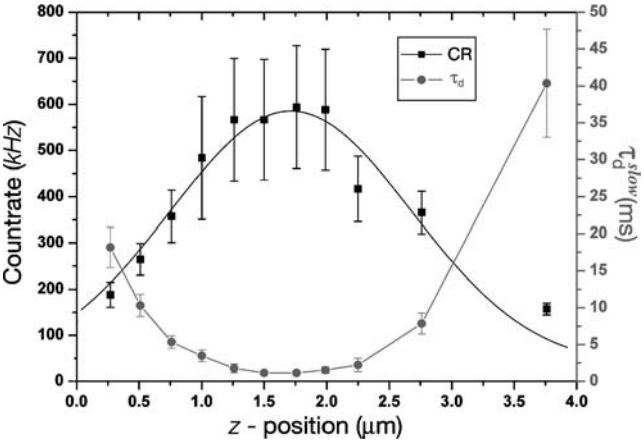

Fig. 3 Dependence of the lateral 2D diffusion-time (τ_d^{slow}), *grey circle points*, and the fluorescence signal $F(t)$ (i.e. countrate CR), *black square points*, versus the relative z-position of the observation volume recorded on the sample n°1. The τ_d^{slow} *error bars* indicate the uncertainty of the diffusion-time, assessed through the autocorrelation curves fitting. At the opposite, the count rate (CR) error bars corresponds to the fluctuation $\delta F(t)$ of the recorded fluorescence signal. The CR experimental data points are well fitted by a Lorentzian profile. Note that the minimum of τ_d^{slow} and the maximum of the count rate occur simultaneously, according to a maximum of fluorescence fluctuation

The mean concentration C can be easily deduced from the mean number of molecules N, according to the simple relation $N = C \times V$, where V is the effective size of the observation optical volume. To avoid any artifact related to the well known modifications of the observation volume profile near the interface glass–water [32–34], we decided to normalize all the concentration values by the total concentration ($C^{fast}+C^{slow}$) for each z position of the observation volume. In consequence, we present in Fig. 4 the evolution of $C^{fast}/(C^{fast}+C^{slow})_z$ and $C^{slow}/(C^{fast}+C^{slow})_z$. Quite obviously, the evolution of the normalized value of both *slow* and *fast* mean concentration reveals clearly the effects of surface hydrophobicity on the dye diffusion (Fig. 4b,c,d). The relative weight of the *slow* 2D diffusion increases with the hydrophobicity degree. For the stronger hydrophobic surface, the $-CH_3$ terminated one (sample 1), the crossover between the two curves (i.e. the concentration evolution of both two classes of dye) moved away to ≈2.5 μm from the surface. Contrarily, for the –OH terminated one, the most hydrophilic surface (sample 3), the influence of the interface becomes significantly residual. Indeed, at the interface only a slight contribution of Rh6G molecules diffusing in two dimensions is observed. It is very interesting to note that the bare coverglass appears as a hydrophobic surface with a long range of the hydrophobic effect, i.e. a 2D diffusion contribution up to 2 μm from the glass–water interface (Fig. 4a). Moreover, whatever the chemical nature of the surface, the influence of the interface globally disappears at about 4 μm and far

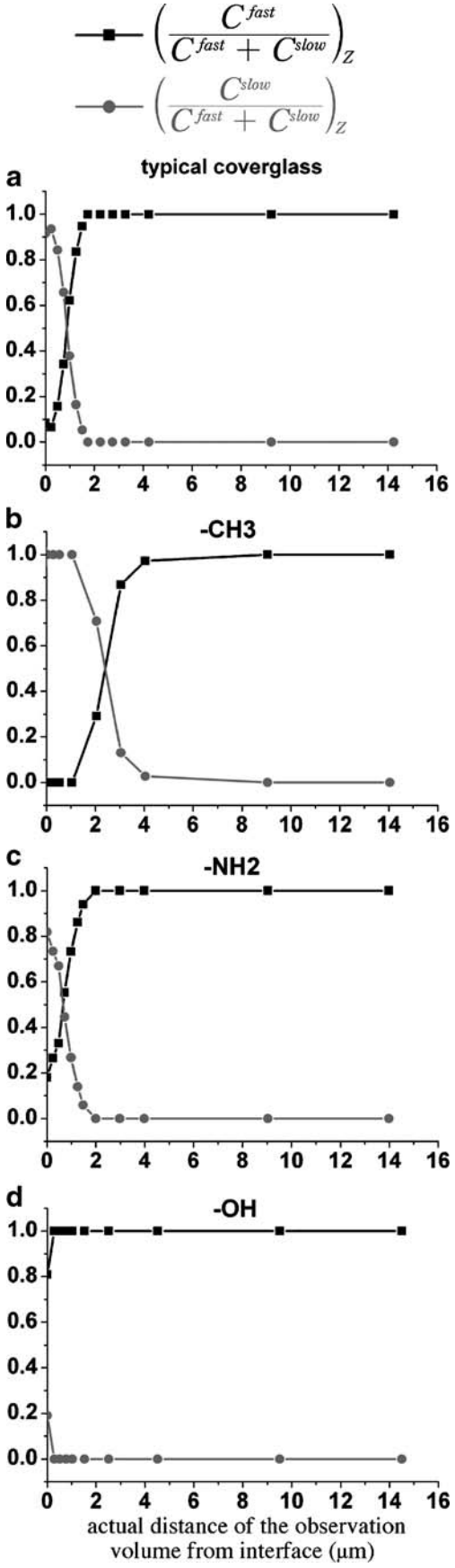

◀ **Fig. 4** Evolution of the normalized value of C^{fast} and C^{slow} (the mean concentration of Rh6G) *vs* the actual distance *z* from interface in regards to different surfaces. *Square black curves*, $C^{fast}/(C^{fast}+C^{slow})_z$. *Circle grey curves*, $C^{slow}/(C^{fast}+C^{slow})_z$. **a** FCS analysis on a bare coverglass. **b**, **c** and **d** FCS analysis on sample n°1, n°2 and n°3, respectively

from the surface we always observed a pure 3D diffusion of the molecules.

Discussions

Interactions between Rh6G, water and the surfaces are directly related to the forces involved. The observations result from the competition between Rh6G and water, Rh6G and surface, water and surface affinities.

The chemical nature of the surfaces has been chosen with different polarity values: $–CH_3$ end group is a typical unpolar surface (with contact angle of 107° with water), –OH end group is on the contrary a high polar surface (with a contact angle <5° with water) and $–NH_2$ end group is a medium polar surface (with contact angle of 67° with water). For this study, Rh6G is a very interesting probe due to its specific interactions with water. Rh6G, as a member of the xanthene dyes family, contains three flat conjugated cycles (chromophoric part, see Fig. 1), which are responsible for the hydrophobicity character of the molecule [35, 36]. But, Rh6G is also a cationic dye which counterbalances the hydrophobic part, thus allowing its solubility in water [35, 36]. These two features are responsible for the slightly solubility of Rh6G in water. It is important to note that this hydrophobicity induces the formation of dimers, in aqueous solutions up to 10^{-6} M [35]. The non-presence of

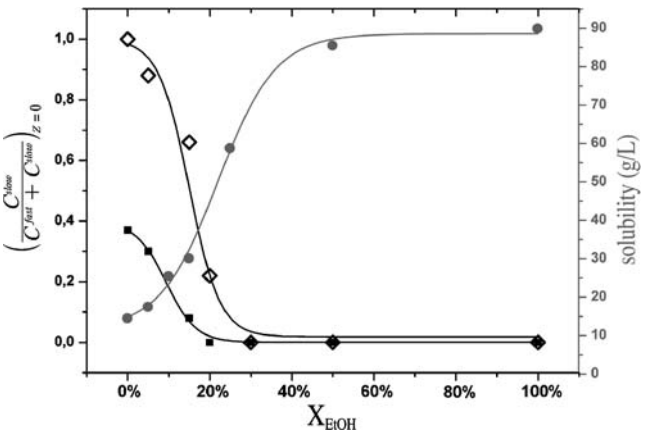

Fig. 5 Fraction of Rh6G molecules diffusing in 2D on the glass–water interface, $C^{slow}/(C^{fast}+C^{slow})_{z=0}$, as a function of ethanol percentage in water solution, X_{EtOH}, by volume. Rhombus empty curves, for $–CH_3$ surface (sample n°1). Square black curves, for the bare coverglass. *Circle grey curves*, Rh6G solubility measurements, assessed by absorption spectroscopy, for the same water–ethanol mix X_{EtOH}

dimers in our nanomolar solution has been checked by recording a single fast diffusion time in water ($\tau_d^{fast} = 44\ \mu s$ for monomers).

As a consequence of the unpolarity of UDTS (–CH_3 end group), the surface is very repulsive for water molecules and then attracts the dyes. Thus, the presence of a large slow 2D diffusion near the –CH_3 surface is caused by strong hydrophobic interactions between UDTS and Rh6G, as shown Fig. 4b. It should be noted that the use of a long alkyl chain (C_{10}) minimized significantly the possible interactions between Rh6G, water and the highly polar silanol groups, which would not have react during the silanization process. The nature of the interactions between Rh6G and unpolar –CH_3 surface is highlighted by the addition of an increasing proportion of an organic solvent, such as ethanol [37]. Thus, we have showed a fast disappearance of this particular affinity that Rh6G molecules have for hydrophobic surface, as presented Fig. 5 for –CH_3 surface and bare coverglass. Indeed, the Rh6G molecules would rather have a preference for ethanol, as show by evolution of their solubility in regards to an enhancement of the proportion of ethanol in water, Fig. 5 (see supporting information section).

On the other hand, at the pH used in our study (≈6.5) and according to the pK_a of primary amine (between 10 and 11), the APDES surface (–NH_2 end group) is protonated. Nevertheless, the weak polarity of the amine groups repulses a part of the water diffusing directly near the surface and then attracts some Rh6G dyes. This attraction is detected by the percentage of Rh6G in water diffusing slowly in 2D on the interface (≈80%), as shown Fig. 4c. On the contrary, the polar SiOH surface is very hydrophilic. The water is then attracted and in spite of the Rh6G is a cationic dye, Rh6G does not react with the surface due to its three flat hydrophobic conjugated cycles. There is a tiny 2D component and FCS measurements reveal only Rh6G diffusing freely in water (3D component), as shown Fig. 4d (actually, at the interface we only observed a few percentage of molecules diffusing in 2D). The same experiment realized with a typical bare coverglass shows that an important proportion of Rh6G is attracted by the surface. The results are similar as the ones recorded for –NH_2 surface, meaning that the bare surface contains other components than silanols.

Note that the axial resolution of our optical device is about 1.5 μm (it corresponds to the axial elongation of the observation volume). The range of the phenomena recorded for the bare coverglass and –NH_2 surface corresponds to this resolution, but for –CH_3 surface the range is longer, ≈4 μm, as shown Fig. 4. This unexpected observation is the consequence of the very strong attraction of Rh6G molecules by unpolar surface. Actually, the attractive force induced by the surface occurs at very short distances, typically below 10 nm from the surface [38], and gives rise to a 2D diffusion of dyes at the vicinity of the glass–water interface. If the number of molecule affected by this attractive force is important (i.e. $N^{slow} \gg N^{fast}$), what one observes in the case of –CH_3 surface, the autocorrelation curves will be consequently dominated by the two-dimensions diffusion (see Eq.(2)). Then, it will be necessary to move away from the surface, at least 1 or 2 μm, in order to no longer collect the fluorescence of this class of molecules. In the case of a high polar surface, such as SiOH, the behavior is completely different. Indeed, when $N^{slow} \ll N^{fast}$, the autocorrelation curves must be governed by the three-dimensions diffusion, as observed on the Fig. 4d.

Conclusion

Fluorescence correlation spectroscopy (FCS) has been used to investigate the influence of the surface hydrophobicity on fluorescent dye diffusion (the often-used Rhodamine 6G). We reported the strong influence of hydrophobic surface on the free diffusion process. This latter is characterized by a slower diffusion time (a 2D process), which only arise at the vicinity of the glass–water interface. We attribute this 2D diffusion of molecules attracted by the surface, due to a competition between molecule–solvent, molecule–surface and surface–solvent affinities. Our investigations have shown a long-range effect in water, up to a few μm from the surface, which increases with the hydrophobicity degree. These new results suggest that FCS measurements near an interface, could be strongly influenced by the chemical nature of the surface and their interpretations could be altered by chemical interactions near the surface.

Supporting information: solubility measurements The solubility of Rh6G has been determined by the usual equilibrium solubility method. A saturated solution of Rh6G has been obtained by stirring an excess of dye in the solvent (different water/ethanol ratio) during 72 h in order to achieve the equilibrium. The saturated solution has been filtered and absorption spectra were done with a UV–Visible spectrometer. The solubility has been calculated using the Beer–Lambert law: $A_{530}=\varepsilon_{530}\ l\ C$. Where A_{530} is the value of the absorbance at 530 nm, ε_{530} the molar extinction coefficient which is 116,000 l mol^{-1} cm^{-1} for Rh6G at 530 nm [39]. l is the path length and C is the concentration of Rh6G molecules in the solution which corresponds to the solubility.

Acknowledgements We authors thank the Région Champagne-Ardenne, France (under the contract "Projet émergence: Spectroscopie

de corrélation de fluorescence en champ proche optique: applications aux biomolécules et biomatériaux") and French National Research Agency (ANR) under the contract "Jeunes Chercheurs JC07_190015".

References

1. Zander CH, Enderlein J, Keller RA (2002) Single molecule detection in solution, methods and applications. Wiley, Berlin
2. Thompson NL, Lakowicz JR (ed) (1991) Topics in fluorescence spectroscopy, vol 1, chapter 6. Plenum, New York
3. Bohmer M, Enderlein J (2003) Fluorescence spectroscopy of single molecules under ambient conditions: methodology and technology. ChemPhysChem 4:792–808
4. Hess ST, Webb WW (2002) Focal volume optics and experimental artifacts in confocal fluorescence correlation spectroscopy. Biophys J 83:2300–2317
5. Jaffiol R, Blancquaert Y, Delon A, Derouard J (2006) Spatial fluorescence cross-correlation spectroscopy. Appl Opt 45:1225–1235
6. Ruckstuhl T, Seeger S (2004) Attoliter detection volumes by confocal total-internal-reflection fluorescence microscopy. Opt Lett 29:569–571
7. Hassler K, Anhut T, Rigler R, Gösch M, Lasser T (2005) High count rates with total internal reflection fluorescence correlation spectroscopy. Biophys J 88:L01–L03
8. Starr TE, Thompson NL (2001) Total internal reflection with fluorescence correlation spectroscopy: combined surface reaction and solution diffusion. Biophys J 80:1575–1584
9. Lenne P-F, Etienne E, Rigneault H (2002) Subwavelength patterns and high detection efficiency in fluorescence correlation spectroscopy using photonic structures. Appl Phys Lett 80(22):4106–4108
10. Ries J, Ruckstuhl T, Verdes D, Schwille P (2008) Supercritical angle fluorescence correlation spectroscopy. Biophys J 94:221–229
11. Rigneault H et al (2005) Enhancement of single-molecule fluorescence detection in subwavelength apertures. Phys Rev Lett 95:117401
12. Wenger J, Rigneault H, Dintinger J, Marguet D, Lenne P-F (2006) Single-fluorophore diffusion in a lipid membrane over a subwavelength aperture. J Biological Phys 32:SN1–SN4
13. Wenger J et al (2007) Diffusion analysis within single nanometric apertures reveals the ultrafine cell membrane organization. Biophys J 92:913–919
14. Levene MJ et al (2003) Zero-mode waveguides for single-molecule analysis at high concentrations. Science 299:682–686
15. Samiee KT, Moran-Mirabal JM, Cheung YK, Craighead HG (2006) Zero mode waveguides for single-molecule spectroscopy on lipid membranes. Biophys J 90:3288–3299
16. Moran-Mirabal JM, Torres AJ, Samiee KT, Baird BA, Graighead HG (2007) Cell investigation of nanostructures: zero-mode waveguides for plasma membrane studies with single molecule resolution. Nanotechnology 18:195101
17. Rigler R, Elson E (2001) Fluorescence correlation spectroscopy, theory and applications. Springer
18. Gösch M, Rigler R (2005) Fluorescence correlation spectroscopy of molecular motions and kinetics. Adv Drug Deliv Rev 57:169–190
19. Krichevsky O, Bonnet G (2002) Fluorescence correlation spectroscopy: the technique and its applications. Rep Prog Phys 65:251–297
20. Rigler R, Mets U, Widengren J, Kask P (1993) Fluorescence correlation spectroscopy with high count rate and low background: analysis of translational diffusion. Euro Biophys J 22:169–175
21. Dittrich P, Schwille P (2002) Spatial two-photon fluorescence cross-correlation spectroscopy for controlling molecular transport in microfluidic structures. Anal Chem 74:4472–4479
22. Wilson T (1993) Fluorescence imaging modes in fibre-optic based confocal scanning microscopes. Opt Commun 96:133–141
23. Wohland T, Rigler R, Vogel H (2001) The standard deviation in fluorescence correlation spectroscopy. Biophys J 80:2987–2999
24. Plain J, Pallandre A, Nysten B, Jonas AM (2006) Nanotemplated crystallization of organic molecules. Small 2:892–897
25. Pallandre A, Glinel K, Jonas AM, Nysten B (2004) Binary nanopatterned surfaces prepared from alkylsilane monolayers. Nano Lett 4:365–371
26. Widengren J, Mets U, Rigler R (1995) Fluorescence correlation spectroscopy of triplet states in solution: a theoretical and experimental study. J Phys Chem 99:13368–13379
27. Lieto AM, Cush RC, Thompson NL (2003) Ligand-receptor kinetics measured by total internal reflection with fluorescence correlation spectroscopy. Biophys J 85:3294–3302
28. Schuster J, Cichos F, Wrachtrup J, von Borczyskowski C (2000) Diffusion of single molecule close to interfaces. Single Mol 1:299–305
29. Benda A, Benes M, Marecek V, Lhotsky A, Hermens WTH, Hof M (2003) How to determine diffusion coefficients in planar phospholipid systems by confocal fluorescence correlation spectroscopy. Langmuir 19:4120–4126
30. Humpolickova J et al (2006) Probing diffusion laws within cellular membranes by Z-scan fluorescence correlation spectroscopy. Biophys J 91:L23–L25
31. Hansen RL, Harris JM (1998) Total internal reflection fluorescence correlation spectroscopy for counting molecules at solid/liquid interfaces. Anal Chem 70:2565–2575
32. Ling H, Lee S-W (1984) Focusing of electromagnetic waves through a dielectric interface. J Opt Soc Am A 1:965–973
33. Török P, Varga P, Booker GR (1995) Electromagnetic diffraction of light focused through a planar interface between materials of mismatched refractive indices: structure of the electromagnetic field. J Opt Soc Am A 12:2136–2144
34. Sick B, Hecht B, Wild UP, Novotny L (2001) Probing confined fields with single molecules and *vice versa*. J Microsc 202:365–373
35. Daré-Doyen S, Doizi D, Guilbaud PH, Djedaini-Pilard F, Perly B, Millié PH (2003) Dimerization of xanthene dyes in water: experimental studies and molecular dynamic simulations. J Phys Chem B 107:13803–13812
36. DelaCruz JL, Blanchard GJ (2003) Understanding the balance between ionic and dispersion interactions in aqueous micellar media. J Phys Chem B 107:7102–7108
37. Hansen RL, Harris JM (1998) Measuring reversible adsorption kinetics of small molecules at solid/liquid interfaces by total internal reflection fluorescence correlation spectroscopy. Anal Chem 70:4247–4256
38. Israelachvili JN (1991) Intermolecular and surface forces, 2nd edn. Academic
39. Brige RR (1987) In Kodak laser dyes, Kodak Publication JJ-169